

博士論文（要約）

A study on the heat pipe for cooling fuel debris in Fukushima Dai-ichi NPP decommissioning

(福島第一原子力発電所廃炉における燃料デブリ
冷却用ヒートパイプに関する研究)

張 瑤

A study on the heat pipe for cooling fuel debris in Fukushima Dai-ichi NPP decommissioning

A dissertation submitted to

The University of Tokyo

In partial fulfillment of the requirements

For the degree of

Doctor of Philosophy

In

Nuclear Engineering & Management

By

Yao ZHANG

July 2019

Advisor: Shunichi Suzuki, Project Professor, Department of Nuclear Engineering and Management

1. Introduction

In the Fukushima accident in 2011, fuel assemblies and core components were damaged, and the fuel debris melted out of Reactor Pressure Vessel (RPV) and fell down at the bottom of the containment vessel. In order to cool down the fuel debris, the water has been injected, which generates a large amount of contaminated water. Suzuki et al. proposed to use geopolymer to cool down and retrieve fuel debris without making contaminated water during Fukushima decommissioning [1]. Geopolymer can provide efficient and practical on-site treatment of radioactive waste streams. It can be used for on-site solidification of highly active materials so that fuel debris can be removed properly. However, geopolymer has a very low heat conductivity, which can be seen as an insulator. Therefore, during the process of applying geopolymer, residual heat must be transferred from fuel debris to outside somehow. The objectives of this study is to develop heat pipes which can be applied in reactors, transferring the heat from fuel debris to the air.

The heat pipe is a highly effective passive device used to transmit heat. Heat pipes allow high transfer rates over considerable distances, with minimal temperature drops, exceptional flexibility, simple construction, and easy control, without a need for external pumping power. Different types of working fluids, such as water, acetone, methanol, ammonia, or sodium can be used in heat pipes based on the required operating temperature [2]. As for the heat pipe to be used in Fukushima decommissioning, water is selected to be the working fluid of heat pipe for safety reasons.

When a heat pipe is used under high dose irradiation, two phenomena would cause its performance differently from the unirradiation condition. One is water radiolysis, the other one is Radiation Induced Surface Activation (RISA) effect. When water radiolysis happens, non-condensable gas such as H_2 and O_2 would be generated in the heat pipe, which will shorten the condensation length and weaken heat transfer [3]. RISA effect is a phenomenon involving the activation of surfaces of metallic oxides attributable to strong affinity for water. When it happens, the contact angle between water and metallic oxides will decrease. That means the capillary force will increase after irradiation, which will enhance the circulation of water and improve the performance of the heat pipe. On the other hand, Gong et al. found that under the same heat flux q , superheat Δt will increase after irradiation [4]. Since convective heat transfer coefficient h equals to $q/\Delta t$, h will become smaller after irradiation. This phenomenon will decrease heat conduction of the heat pipe. Hence, these two opposite effects needs to be studied. For the pipe wall material, it had better be hydrophobic to enhance the heat pipe performance. For the wick structure material, it had better be hydrophilic to obtain a better circulation of water.

When heat pipes are set up in the geopolymer to remove the residual heat in the containment vessel, the influence of radiation environment to heat pipes should be studied. The heat pipe heat removal system is shown in Fig.1. (L_e is evaporation length, L_a is adiabatic length, and L_c is condensation length.)

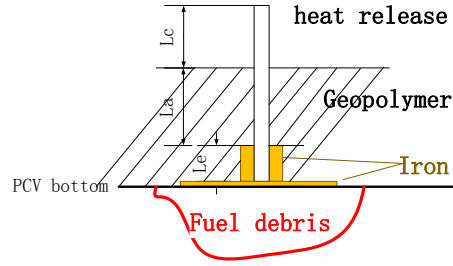


Fig.1 The heat pipe heat removal system

The maximum heat transfer coefficient of the heat pipe can be expressed by equation (1) [5]:

$$(QL)_{c,max} = 2 \cdot \left(\frac{K}{r_c}\right) \cdot A_w \cdot \left(1 + \frac{\rho_l \cdot L \cdot \sin\beta}{2\sigma_l/r_c}\right) \left(\frac{\rho_g \cdot \sigma \cdot \lambda}{\mu_l}\right) \quad (1)$$

In which K is the permeability of the wick and r_c is the effective radius of the wick, these two parameters are very important for the heat pipe performance. β is the inclination angle of the heat pipe. A_w is the cross section area of the wick. L is the length of the heat pipe. These parameters can be changed by engineering considerations. σ is the surface tension of working fluid. ρ is the density of working fluid. μ is viscosity coefficient. These are the fixed values.

A summary of the workflow is shown in Fig.2.

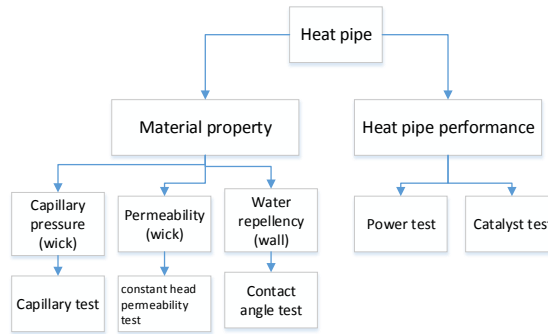


Fig.2 Workflow

2. Material properties

2.1 contact angle test

According to references [6], the superhydrophobic metal surface by producing the hierarchical nano/microstructure with femtosecond laser pulses can be obtained. In this test, copper plates with 6 kinds of surface roughness were tested: 80#, 400#, 1000#, 1500# abrasive paper respectively treated copper and 510nm and 1030 nm laser treated copper surface by the amplified Ti:sapphire laser system. The laser treated copper samples are textured with an array of parallel microgrooves covered by extensive nanostructures.

Droplet tests were performed on these surfaces and measured the contact angle. By a high speed camera, the droplet images on different copper surfaces were obtained, and the contact angle between the copper plate and the droplet was measured. The results are shown in Fig.3. Abrasive paper treated surface is hydrophilic; Laser treated surface is hydrophobic. The surface treated by

1030nm laser is more hydrophobic than 515nm laser. For the water repellent pipe wall, hydrophobic surface is needed.

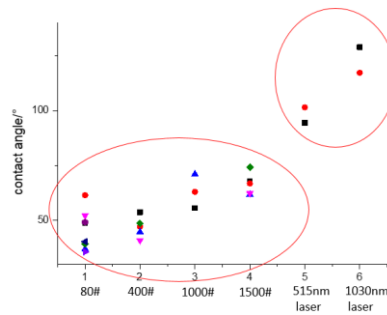


Fig.3 Contact angle of different surfaces

2.2 Capillary Test

The outline of the capillary test is shown in Fig.4, where the equation is shown as below:

$$r = \frac{2\sigma \cos\theta}{\rho gh} \quad (2)$$

in which, r is effective radius, σ is surface tension at room temperature (0.072N/m), h is the capillary rise.

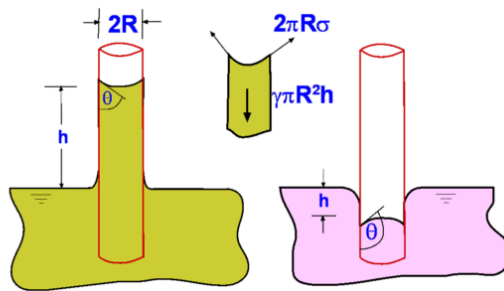


Fig.4 The outline of the capillary test

Different wick materials were put into fine glass tubes ($\Phi 1\text{mm}$) and then the heights of the water rising in the glass tubes were observed. There are two kinds of wick samples. One is NASLON filter (filtration diameter 1-120 μm), made of SUS316L, the other is 7 μm polyacrylonitrile based carbon fiber (filament number 1500). The capillary rise results and calculated effective radius are shown in Table 1.

Table 1 Capillary results

	Capillary rise (cm)	Effective radius(μm)
No filling	1	—
SUS mesh	13	122
Carbon fiber	32.5	45

2.3 Permeability Test

In laminar flow conditions, the rate of flow through the cross section area of porous medium under hydraulic gradient is defined as the coefficient of permeability. The permeability coefficient test is

shown in Fig.5. For a constant head h , coefficient of permeability K can be calculated as QL/Ah . The test facility parameters are shown in Table 2. There are two test samples in permeability tests. One is NASLON filter mesh made of SUS316L, the other is polyacrylonitrile based carbon fiber mesh.

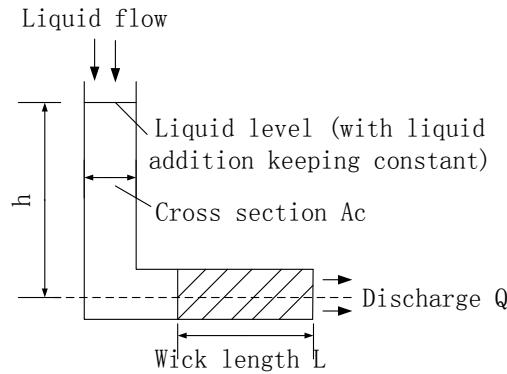


Fig.5 The facility schematic diagram of permeability coefficient test

Table 2 Parameters of permeability test facility

	Experiment facility value
Constant head h	42.5 cm
Wick length L	5 cm
Cross section A_c	0.79 cm ²

$$\text{Permeability coefficient } K = QL/Ah; \quad (3)$$

$$\text{Permeability } K' = \mu K / \rho g \quad (4)$$

$$(\mu = 1.005 \cdot 10^{-3} \text{ Pa}\cdot\text{s})$$

Discharging water was measured and permeability K' for different wick materials were calculated, shown in Table 3.

The effective radius of the SUS mesh is smaller than that of the carbon fiber. The permeability of the SUS mesh is larger than that of the carbon fiber.

Table 3 permeability test results

	Density ρ (g/cm ³)	Discharge Q (cm ³ /sec)	Permeability Coefficient K (cm/s)	Permeability K' (m ²)
SUS mesh	0.52	1.82	0.273	$2.8 \cdot 10^{-10}$
Carbon fiber mesh	0.32	0.375	0.056	$0.58 \cdot 10^{-10}$

For the value of K/r_c , the value of the SUS mesh is larger than that of the carbon fiber. With a larger value of K/r_c , the performance of the heat pipe is better. However, the permeability of the

carbon fiber can be changed because it relates to density. With smaller density of the carbon fiber, the permeability will become larger. Meanwhile, the effective radius wouldn't change because density is not a key factor for capillary rise. Therefore, the carbon fiber makes a good wick candidate because of its high capillarity.

3. Heat pipe test

3.1 test facility

The heat pipe test system is shown in Fig.6. The heat source in this system is a copper block with two heaters inserted. The heat sink here is a peltier unit. The peltier effect is the direct conversion of temperature differences to the electric voltage. It creates a heat flux between the junctions of two different types of materials. When the current flows through a loop of different conductors, heat absorption and release will occur at the junctions with different current direction. Glass wool was used as the insulator for the copper block, the peltier unit and the adiabatic section of the heat pipe. The length of the heat pipe is 500mm. The evaporator section and condensation section is 100mm respectively. The adiabatic section in the middle is 300mm. To evaluate the heat pipe performance more precisely, the heat transfer power of each heat pipe was calculated. Firstly, the total power of DC power supply for the copper block was measured. Heat loss was measured in each case. Then, the heat pipe power can be calculated by subtracting the heat loss from DC power. Repeated tests were done three times in each case.

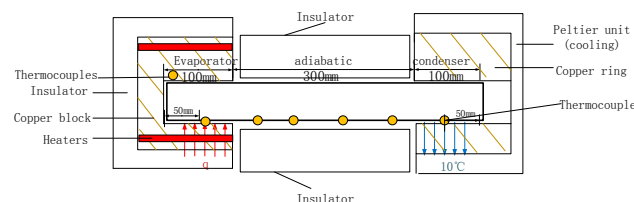


Fig.6 Schematic of heat pipe test system

3.2 The fabricating process of heat pipe

The heat pipe contains a heat pipe shell, a wick structure, and working fluid (water). In the fabricating process, strings of carbon fiber were attached to the SUS inner structure, combining as the wick. Then, the assembled wick was put into the pipe. At last, the working fluid was injected in the pipe.

3.2.1 Inner structure

The cross section of the inner structure is star-shape, as Fig.7 shows, to increase the contact surface area. Two inner structures with different lengths were used and the temperature distribution of the heat pipes were compared to find out the suitable structure by using peltier units at both ends. The pipe shell is 50cm long. Two candidates of the inner structure are 30cm and 48cm long respectively. For the 30cm inner structure, the inner structure was put in the middle and 10cm SUS coiling structures were put at each end of the pipe. The two inner structures are compared in Fig.8.

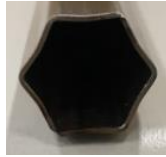


Fig.7 The cross section of the inner structure



Fig.8 two inner structures

Thermocouples were attached along the heat pipe wall at the length of 50cm, 150cm, 250cm, 350cm and 450cm to obtain the temperature distribution of the two heat pipes. The evaporator section and condensation section of the heat pipe were 100mm respectively. The results are shown in Fig.9.

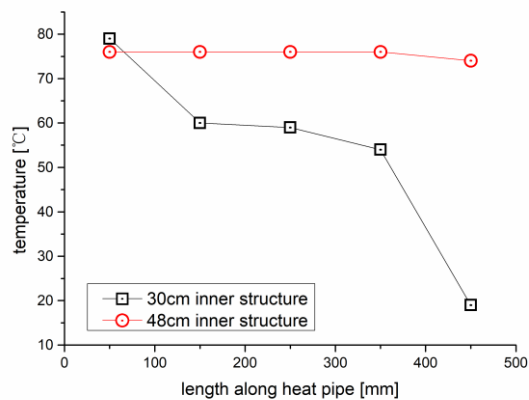


Fig.9 Temperature distribution

From the results above, the one with the 48cm inner structure works as a functional heat pipe. For the one with the 30cm inner structure, the evaporator and condenser section is likely to suffer an obvious temperature decrease. Even for the evaporator and condenser section, the heat pipe needs a wick structure to keep the working fluid circulate and transfer the heat.

3.2.2 Assembling process

Strings of carbon fiber (4.2g in total) were attached to 48cm inner structure, combining as the wick. 15.5ml water (10% of the pipe volume) were injected inside the pipe. After that, dry ice was applied to make a vacuum condition inside the pipe. Because under room temperature, the water would become vapor with the inner pressure decreasing. To make the internal pressure lower than 100Pa, the temperature of the working fluid should be below -21°C. Therefore, dry ice (melting point -78.5°C) was used.

3.2.3 Test results of the reference HP

With this experimental setup, the evaporator section was kept at 60°C and the condenser section was kept at 10°C. The voltage and the current of the heaters were measured by a digital DC power supply and a non-contact DC galvanometer.

The heaters' power supply was working discontinuously, to keep the evaporator section at the constant temperature of 60°C. The current is the average value of current during the stable state time.

Heat pipe power $P = P_{total} - P_{heat\ loss}$;

$P_{total} = IU$, in which I is the current and U is the voltage of the heaters; $U = 60V$, $I = 0.77A$.

$P_{heat\ loss} = 1.7W$ in this case. $P_{heat\ loss}$ is obtained by a SUS heat pipe shell under the same experimental condition and procedure as the heat pipe.

The power of the functional heat pipe was calculated as 44.7W. The temperature distribution along the heat pipe is shown in Fig.10.

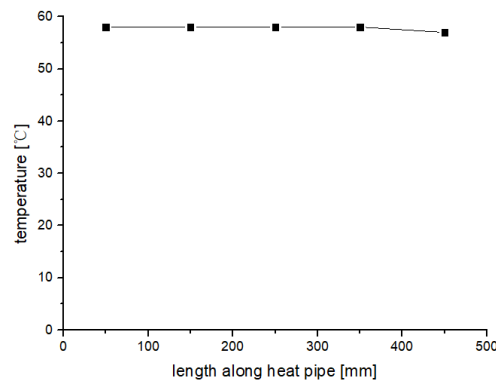


Fig.10 Temperature distribution

3.3 gamma ray tests

3.3.1 Commercial HP test

Firstly, the existing commercial copper heat pipes with grooves inside were irradiated and tested. The tested copper heat pipe is 300 mm long and the outer diameter is 12.7 mm. The inner diameter of the peltier unit is 25.4 mm. Therefore copper ring with the outer diameter of 25.4 mm and the inner diameter of 12.7 mm was used. One heat pipe was irradiated under gamma irradiation, and the total dose was 1445kGy. Heat pipe performance tests were done by using this irradiated heat pipe and an unirradiated heat pipe.

With an 80°C heat source and a 20°C heat sink, the temperature distribution is shown in Fig.11.

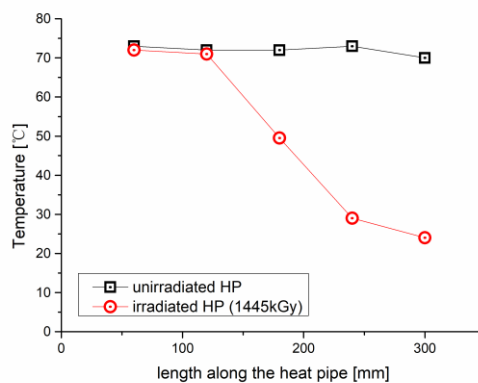


Fig.11 Temperature distribution

The irradiated heat pipe suffers performance degradation obviously, since noncondensable gas may accumulate inside the heat pipe because of water radiolysis. The gas composition inside the heat pipe was measured. The heat pipe under 1445 kGy irradiation was cut and examined. The volume concentration of the gas inside the heat pipe is 89% hydrogen and 3.3% oxygen. Judging from the temperature distribution, the condenser section didn't work functional because noncondensable such as hydrogen was accumulated in this section during the heat pipe test. Therefore, catalyst should be applied in the condenser section of the heat pipe.

3.3.2 Catalyst design

When heat pipes are used under high irradiation environment, noncondensable gas keeps accumulating inside as irradiation dose increases. Therefore, a mechanism to suppress the gas is necessary to use for the water-based heat pipe under high irradiation. Palladium is used as the catalyst to promote hydrogen and oxygen recombination into water. Eight heat pipes with different configuration were designed as Table 4 shows. The length of inner structure, catalyst, and water amount were studied independently as parameters.

Table 4 Heat pipes with different configuration

Sample	Inner structure /cm	catalyst	Water amount
S1	48	No catalyst	10%
S2	48	Honeycomb H1	10%
S3	48	Honeycomb H2	10%
S4	48	No catalyst	5%
S5	43	No catalyst	10%
S6	48	Pd wire/Pd plate	10%
S7	48	Pd powder	10%
S8	43	Pd wire/Pd chain	10%

For sample S2 and S3, Honeycomb H1 and H2 is shown in Fig.12. The surface is coated by palladium. The structure of the honeycomb was introduced to get a larger contact surface area between gas and the structure with less pressure drop.



Fig.12 Honeycomb H1 and H2

For S7, palladium powder in water was used because of less generation of hydrogen by water radiolysis.

For S6, 2m palladium wire was used. Also, a palladium plate at the end of cap was applied (Fig.13).

For S8, a chain structure was made by palladium strips and 1m palladium wire (Fig.14). The chain

structure was introduced to get a larger contact surface area with hydrogen.



Fig.13 the catalyst in S6 Fig.14 the catalyst in S8

3.3.3 results

Heat pipes S1-S8 were irradiated under gamma ray. The performance of heat pipes S1-S8 at different irradiation dose is shown in Fig.15.

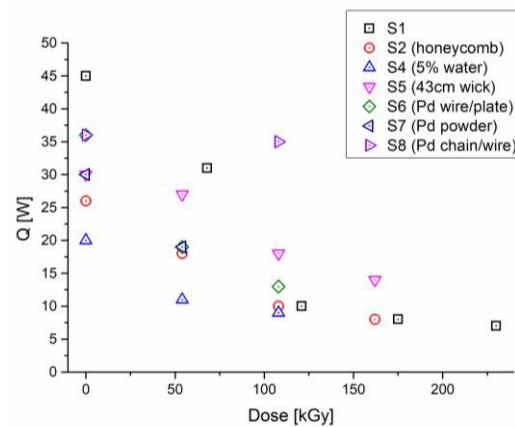


Fig.15 Heat pipe power at different irradiation dose

S2 and S3 doesn't perform well even before the irradiation, because the pressure drop is affected by the honeycomb structure.

The water amount of S4 was reduced to 5%, but S4 didn't have a very good performance either. It may reach the limit of dry out because of the lack of the working fluid.

S6 and S7 didn't perform well after 54kGy gamma ray irradiation, probably because the catalyzing space was not big enough for the accumulated hydrogen.

S5 was introduced for a bigger space to reserve the noncondensable gas. It performed well after 54kGy irradiation, but failed after 108 kGy irradiation.

Finally, heat pipe S8, with a bigger gas reservoir space and the palladium catalyst on the top, kept a good performance even after 108kGy irradiation.

4. Conclusion

In this paper, the radiation effect on the heat pipe was studied. For the pipe wall material, it had better be hydrophobic to enhance the heat pipe performance. For the wick material, permeability

and effective radius are key parameters to enhance the performance of the heat pipe. Permeability tests and capillary tests were done for two candidate wick materials as the SUS mesh and the carbon fiber. The effective radius of the SUS mesh is smaller than that of the carbon fiber, while the permeability of the SUS mesh is larger than that of the carbon fiber. Carbon fiber makes a good wick candidate because of its high capillarity.

For the heat pipe tests, different heat pipes with different catalyst were made. The performance of different heat pipes under different irradiation dose were respectively measured. The irradiated heat pipe suffers performance degradation of heat transfer power because of accumulated noncondensable gas after irradiation. The heat pipe with the 43cm inner structure and the palladium catalyst on the top has the best performance among all the heat pipes, whose power barely changed up to 108kGy. Other heat pipes suffered obvious performance degradation after 54kGy. Under gamma ray irradiation condition, commercial groove heat pipes couldn't work functionally. A suitable heat pipe under gamma irradiation was newly proposed in this study.

References

- [1] S Suzuki, K Okamoto, A new method of fuel debris retrieval with geopolymer for Fukushima Dai-ichi NPP[C]. 14th Annual conference of Japan Society of Maintenology, 2017.
- [2] Faghri, Amir. "Review and advances in heat pipe science and technology." *Journal of HeatTransfer* 134.12 (2012): 123001.
- [3] Kinsho M, Ogiwara N, Masukawa F, et al. Gamma-ray irradiation experiments of collimator key components for the 3GeV-RCS of J-PARC[C]//Particle Accelerator Conference, 2005.PAC 2005. Proceedings of the. IEEE, 2005: 1309-1311.
- [4] Gong H, Khan A R, Erkan N, et al. Critical heat flux enhancement in downward-facing pool boiling with radiation induced surface activation effect[J]. *International Journal of Heat & Mass Transfer*, 2017, 109:93-102.
- [5] Peterson G P. An introduction to heat pipes: modeling, testing, and applications[J]. 1994.
- [6] Vorobyev, A. Y., and Chunlei Guo. "Multifunctional surfaces produced by femtosecond laser pulses." *Journal of Applied Physics* 117.3 (2015): 033103.